ELSEVIER

Journal of Molecular Catalysis A: Chemical 153 (2000) 109–119

JOURNAL OF MOLECULAR CATALYSIS A: CHEMICAL

www.elsevier.com/locate/molcata

Homopolymerization of ethylene and copolymerization of ethylene and 1-hexene with bridged metallocene/methylaluminoxane catalysts: the influence of the bridging moiety

Alexander Köppl, Andrea I. Babel, Helmut G. Alt *

Laboratorium für Anorganische Chemie, Universität Bayreuth, D-95440 Bayreuth, Germany

Received 30 March 1999; received in revised form 17 June 1999; accepted 9 August 1999

Abstract

Ethylene and 1-hexene have been copolymerized with the catalyst system 9-fluorenylidene-1-cyclopentadienylidene-2-hex-5-enylidene zirconium dichloride/PHT (PHT = partially hydrolyzed trimethylaluminum). The resultant polymer has been characterized. The product of the copolymerization parameters $r_1 \cdot r_2$ indicates a statistical distribution of the monomers in the produced poly(ethylene-co-1-hexene). Various *ansa*-bis(fluorenylidene) and *ansa*-fluorenylidene cyclopentadienylidene zirconium dichloride complexes have also been used as catalyst precursors to homopolymerize ethylene and copolymerize ethylene and 1-hexene heterogeneously. For these reactions, the relationships between ''bite-angle'', polymerization activity, and comonomer incorporation have been investigated using PHT/silica gel and MAO/silica gel as aluminoxane type cocatalysts. The effect of comonomer on the catalytic activity is generally positive for MAO/silica gel catalysts and negative for PHT/silica gel catalysts.

Keywords: Copolymerization; Metallocene catalysts; Supported PHT

1. Introduction

Olefin copolymers are commercially very significant. In specific, ethylene/α-olefin copolymers have production volumes that are greater than those of homopolymers. Metallocene polymerization technology offers new ways to produce these olefin copolymers with special properties [1–4]. Linear Low-Density Polyethylene (LLDPE) is synthesized by the copolymerization of ethylene with 1-butene, 1-hexene or 1-octene [5]. LLDPE contains regularly distributed short chain branches that decrease resin crystallinity and density imparting beneficial mechanical properties. Many new resin applications are addressed by using different comonomers [6–8] or combinations thereof. Here, we report the heterogeneous metallocene catalyzed copolymerization of ethylene and 1-hexene using aluminoxane type cocatalysts.

* Corresponding author. Fax: +49-921-552157; e-mail: helmut.alt@uni-bayreuth.de

1381-1169/00/$ - see front matter
PII: S1381-1169(99)00310-6

2. Results and discussion

Two types of metallocene catalyst precursor were used in the polymerization experiments. Type A represents an *ansa*-bis(fluorenylidene) zirconium dichloride complex (Fig. 1). The *ansa*-fluorenylidene-cyclopentadienylidene zirconium dichloride complex of type B is shown in Fig. 2.

2.1. Synthesis of the catalysts

The heterogeneous polymerization catalyst (M)/PHT [9] is synthesized as shown in Scheme 1. The essential difference to known procedures [10–14] of forming heterogeneous metallocene/MAO (methylaluminoxane) catalysts is the order of water addition required for the synthesis of the MAO type cocatalysts. Using this procedure, it was possible to immobilize the methylaluminoxane type cocatalysts (Scheme 1) [9] completely on non-polar support materials, for example activated carbon or polyethylene or on polar materials like starch or cellulose. In a second series of measurements, the catalyst precursors were activated analogous to Scheme 2.

2.2. Copolymerization of ethylene and 1-hexene with a catalyst precursor of type B (X = 2-hexenylidene) [15]

The properties of the copolymers do not only depend on the comonomer content but also on the distribution of the comonomers in different polymer chains and within each individual chain. If the comonomer has a block-like distribution at either the inter- or intramolecular level, the polymer may still contain significant crystalline areas even at relatively high comonomer contents. In contrast, if there is a more random distribution of the comonomer, a less crystalline copolymer is obtained at an equivalent comonomer content.

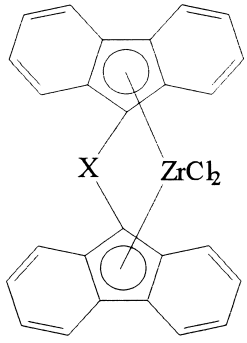

Fig. 1. *Ansa*–metallocene complex: type A, X = bridging moiety.

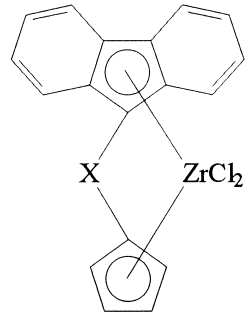

Fig. 2. *Ansa*–metallocene complex: type B, X = bridging moiety.

2.2.1. Determination of the copolymerization parameters

The insertion rate of monomer and comonomer which is specific for each catalyst, is generally described with two copolymerization parameters, r_1 and r_2. These parameters are based on various mathematical models that describe the copolymerization behavior of Ziegler–Natta catalysts, although it was originally developed for radical copolymerization reactions. The model used is that of the copolymerization parameters by Mayo and Lewis [16]. If the copolymerization parameters of a given catalyst and the starting monomer/comonomer molar ratio are known, the polymer composition and the sequence distribution of the monomers in the copolymer can be calculated. Thus the complete microstructure of the polymer is predictable. The product $r_1 \cdot r_2$ is an indicator for the distribution of the monomers within a polymer chain. While catalysts with $r_1 \cdot r_2 > 1$ are inclined to insert comonomer in block-like segments, the ones with $r_1 \cdot r_2 < 1$ produce resins with isolated comonomer units. In the special

Scheme 1. General synthesis of the heterogeneous metallocene catalyst ''support–PHT–M'' (M = metallocene complex, support = silica gel, polyethylene).

Scheme 2. Synthesis of a silica gel/MAO based heterogeneous metallocene catalyst.

case of $r_1 \cdot r_2 = 1$, the insertion rate is independent of the last inserted olefin. Then, the comonomer distribution corresponds to a Bernoulli-random distribution. The copolymerization parameters for the PHT/silica gel catalyst system were determined according to the method of Fineman and Ross [17]: $r_1 = 32.14$, $r_2 = 0.027$, $r_1 \cdot r_2 = 0.87$. Since the $r_1 \cdot r_2$ product is less than one, it confirms a random comonomer distribution in the polymer chain. This result is typical for metallocene catalysts (Table 1). This observed behavior corresponds to an ideal, non-azeotropic copolymerization with $r_1 = 1/r_2$, i.e., $k_{11}/k_{12} = k_{21}/k_{22}$.

2.2.2. Influence of the comonomer content on the polymer properties

When the concentration of 1-hexene in an ethylene copolymerization reactor exceeds 30 mol% of the total reactor olefin content, the process is commercially unattractive due to the expense required to remove the unreacted 1-hexene from the polymer particles. Therefore, studies of the activity and resin molecular weight M_η in this report were limited to the range between 0–15 mol% 1-hexene content in the monomer mixture (Scheme 3). PHT/metallocene complex type B (X = 2-hexenylidene), was used as catalyst system.

Table 1
Copolymerisation parameters r_1 and r_2 for ethylene and a second α-olefin [18,19]
Ind = indenylidene, Flu = fluorenylidene, ^{i}Pr = isopropylidene.

Catalyst	r_1	r_2	$r_1 \cdot r_2$
δ-$TiCl_3$/$AlEt_3$	7.3	0.76[a]	5.5
SiO_2/$MgCl_2$/$TiCl_4$/AlEt3	5–10	0.2–0.34[a]	1.9
Cp_2ZrCl_2/MAO	48	0.015[a]	0.72
Flu(2,2-^{i}Pr)CpZrCl_2/MAO	1.3	0.20[a]	0.26
Ind_2(1,1-$SiMe_2$)ZrCl_2/MAO	25	0.016[b]	0.4

[a] Ethylene/propylene.
[b] Ethylene/1-hexene.

Catalyst productivity and polymer molecular weight are already significantly influenced at relatively low 1-hexene concentrations. For numerous metallocene catalyzed polymerization reactions, as for example in the system bis(1-indenylidene)(1,2-ethylidene) zirconium dichloride/MAO [20], the catalyst productivity is increased when butene or a longer chain α-olefin is used as a comonomer. However, in the present case, a ''negative comonomer effect'' was observed, i.e., the catalyst productivity decreased with the addition of 1-hexene. Sporadically appearing regional errors might be responsible for this copolymerization behavior [21–26]. They are caused by the 2,1-insertions instead of the preferred 1,2-insertions. Investigations by Busico et al. [26] revealed that insertions into a secondary Zr-alkyl moiety occur approximately 100 times slower than insertions into a primary Zr-alkyl moiety. Thus, 2,1-insertions at a frequency of 1% are sufficient to trap 90% of the catalyst centers in secondary Zr-alkyl moieties (Scheme 4).

Scheme 5 illustrates the dependency of the melting point T_m and the crystallinity degree α on the 1-hexene content of the monomer mixture. T_m as well as α decrease with increasing 1-hexene concentration. Butyl short chain branches are formed by the insertion of 1-hexene into the polymer decreasing the melting point and crystallinity of the copolymer.

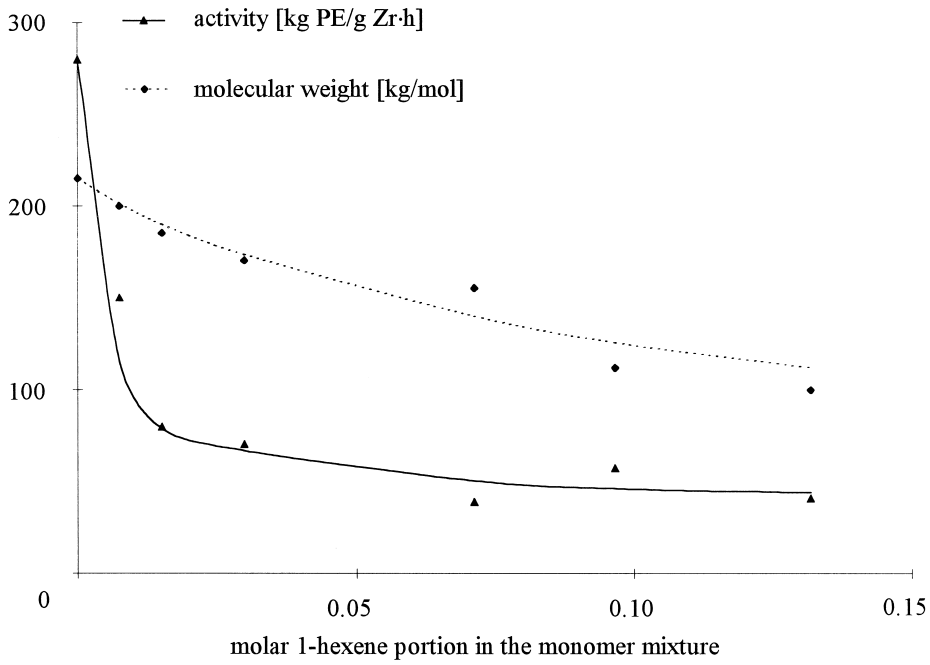

Scheme 3. Dependency of the molecular weight and the activity on the 1-hexene portion in the total olefin content. Polymerization conditions: 10.0 bar ethylene pressure, 500 ml *n*-pentane, 1.0 ml TIBA (1.6 M in *n*-hexane), 70°C, Al:Zr = 260:1, Al:O = 1.44:1, catalyst precursor: metallocene complex type B (X = 2-hexenylidene), polyethylene portion in the catalyst: 36%, 1-hexene is added in one portion into the reactor.

2.2.3. Comonomer influence on the kinetics of the polymerization process

In Section 2.2.2, the influence of comonomer on the catalyst and polymer properties was investigated in detail. Accordingly, the crystallinity of poly(ethylene-co-1-hexene) decreases drastically with increasing comonomer content. If the active center is shielded by a thick, crystalline polyethylene shell, the crystallinity of the polymer can have significant influence on the kinetics of the polymerization reaction. One explanation for decreases in catalyst activity with increasing polymerization time is that diffusion of the monomer to the active catalyst center is inhibited by the growing mass of polymer.

A significantly lower crystallinity due to short chain branches may inhibit the formation of a crystalline polymer shell around the catalyst center so that a more constant growth rate is observed. Scheme 6 illustrates the kinetic profiles of the homopolymerization of ethylene and the copolymerization of ethylene and 1-hexene with the PHT/metallocene complex type B (X = 2-hexenylidene) catalyst system. The difference in the slope of both curves at the beginning of the reaction is clearly recognizable. The homopolymerization proceeds at least at the beginning of the reaction without activity loss, while the copolymerization exhibits even at the beginning, a slower reaction rate. Therefore, this may suggest that 1-hexene forms a second type of active polymerization site providing a significantly slower growth rate.

2.3. Influence of the bridging moiety on the catalytic properties: homopolymerization of ethylene

The type and size of the bridging moiety significantly influences the polymerization and copolymerization behavior of *ansa*-fluoren-

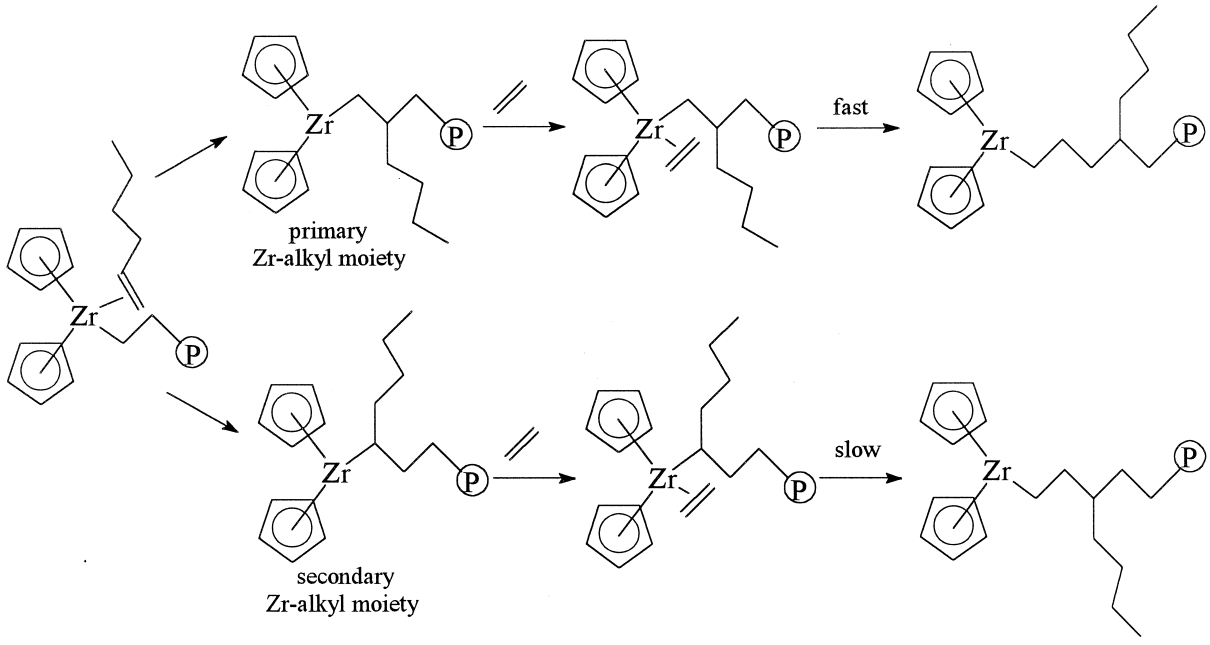

Scheme 4. Comparison of the insertion rates for primary and secondary Zr-alkyl moieties.

ylidene cyclopentadienylidene and *ansa*-bis(fluorenylidene)zirconium dichloride complexes [27–29]. The direct dependency of ''bite-angle'' on the bridging element of the π-ligands eluci-

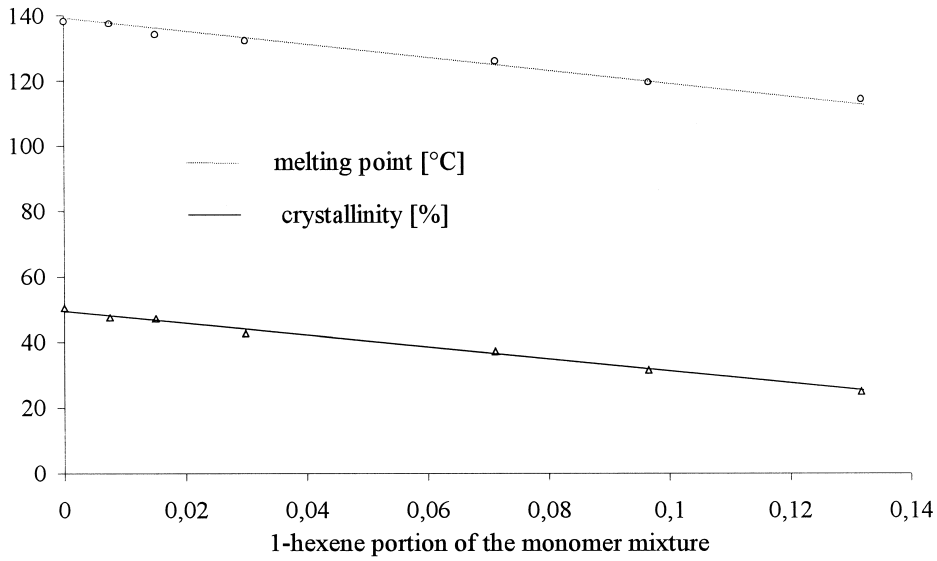

Scheme 5. Dependency of melting point and crystallinity of the produced polymer on the molar 1-hexene portion of the monomer mixture. polymerization conditions: 10.0 bar ethylene pressure, 500 ml *n*-pentane, 1.0 ml TIBA (1.6 M in *n*-hexane), 70°C, Al:Zr = 260:1, Al:O = 1.44:1, catalyst precursor: metallocene complex type B (X = 2-hexenylidene), polyethylene portion in the catalyst: 36%, 1-hexene is added in one portion into the reactor.

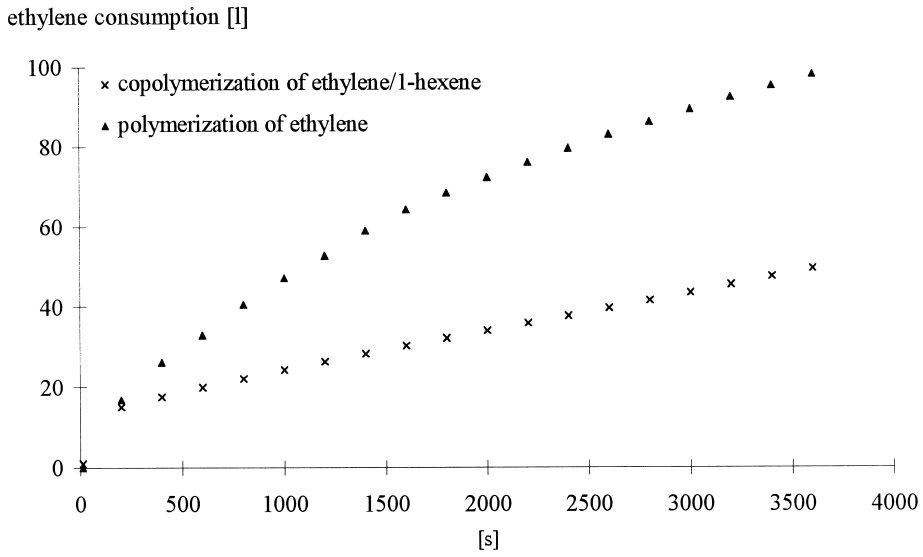

Scheme 6. Kinetic profiles for the homopolymerization of ethylene and the copolymerization of ethylene and 1-hexene. polymerization conditions: 10.0 bar ethylene pressure, 500 ml *n*-pentane, 1.0 ml TIBA (1.6 M in *n*-hexane), 70°C, Al:Zr = 260:1, Al:O = 1.44:1, catalyst precursor: metallocene complex type B (X = 2-hexenylidene), polyethylene portion in the catalyst: 36%, 1-hexene is added in one portion into the reactor.

dates the reason for this behavior in the case of the *ansa*-bis(fluorenylidene) zirconium dichloride complexes studied. The optimized structures from MM2/Cerius2/Universal1.01 calculations were used.

A larger ''bite angle'' (Scheme 7) should allow better access of the monomer to the metal cation. Therefore, catalyst precursors with wider dihedral angles should exhibit higher activities at comparable stability. However, different dihedral angles also influence the electron density on the metal and, therefore, the stability of *ansa*-metallocene dichloride complexes. On the one hand, ligand systems with a larger opening angle and a lower electron density on the center metal atom should exhibit higher activity, on the other hand, their thermal stability decreases in the same order. Decreased stability should lead to a loss in catalytic activity. The investigated metallocene dichloride complexes were either immobilized on silica gel/PHT (Scheme 1) or on silica gel through deposition of a homogeneous metallocene/MAO solution (Scheme 2). Table 2 summarizes the polymerization results for the various *ansa*-bis(fluorenylidene) complexes studied. The C_2-bridged metallocene complex type A ($x = (CH_2)_2$) exhibits the highest activity for both catalyst systems (**5**/**6**), while the analogous Si_2-bridged catalyst precursor with the narrowest dihedral angle exhibits the lowest activity as expected (**7**/**8**). The exceptional activity of metallocene complex type A ($x = (CH_2)_2$) is a reflection of the thermal and chemical stability of this com-

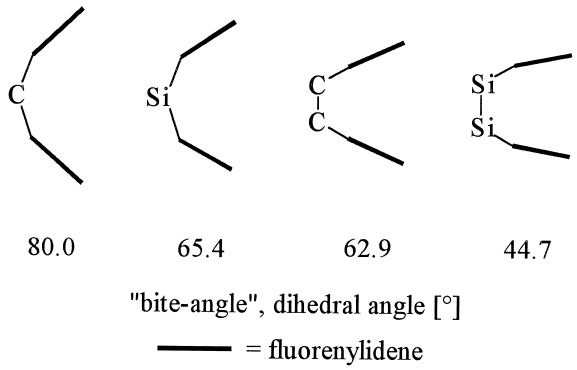

Scheme 7. Schematic representation of the influence of the bridging moiety on the ''bite-angle'' in *ansa*-bis(fluorenylidene) zirconium dichloride complexes (type A).

Table 2
Polymerization results of various *ansa*-bis(fluorenylidene) complexes activated with SiO_2/PHT and SiO_2/MAO
Polymerization conditions: SiO_2/PHT: 10.0 bar ethylene pressure, 500 ml *n*-pentane, 1.0 ml TIBA (1.6 M in *n*-hexane), 70°C, Al:Zr = 260:1, Al:O = 1.44:1, silica gel portion in the catalyst: 36%; SiO_2/MAO: 10.0 bar ethylene pressure, 500 ml *n*-pentane, 70°C, Al:Zr = 2500:1, 2.0 g SiO_2 silica gel.
C_5 = pentylidene.

Catalyst precursor/cocatalyst	Activity (kg PE/g Zr h)	PE — M_η (kg/mol)	PE — $T_{m,1}$, $T_{m,2}$ (°C)	PE — $\Delta H_{m,1}$, $\Delta H_{m,2}$ (J/g)	PE — α (%)
Type A (X = 1,1-C_5)/SiO_2/PHT (**1**)	34	470	103.6, 134.3	3.3, 130.8	45
Type A (X = 1,1-C_5)/SiO_2/MAO (**2**)	114	400	137.1	148.0	51
Type A (X = $SiMe_2$)/SiO_2/PHT (**3**)	110	320	140.0	145.4	50
Type A (X = $SiMe_2$)/SiO_2/MAO (**4**)	126	330	138.2	143.1	49
Type A (X = $(CH_2)_2$)/SiO_2/PHT (**5**)	120	415	139.1	165.5	57
Type A (X = $(CH_2)_2$)/SiO_2/MAO (**6**)	275	480	136.4	141.5	49
Type A (X = 1,2-Me_2Si-$SiMe_2$)/SiO_2/PHT (**7**)	12	120	141.0	183.7	63
Type A (X = 1,2-Me_2Si-$SiMe_2$)/SiO_2/MAO (**8**)	33	70	135.2	167.4	58

pound [27]. The C_1-bridged metallocene complex type A (x = 1,1-pentylidene) (**1**/**2**) is relatively unstable and, despite its large dihedral angle, has a low activity. In all cases, the silica gel/MAO catalyst system has higher activities than the analogous silica gel/PHT system. However, the higher productivities for the silica gel/MAO catalyst system are achieved at a ten fold higher aluminum–zirconium molar ratio. However, the difference varies remarkably depending on the catalyst precursor. With the exception of the C_2-bridged catalyst precursor **5**/**6**, the molecular weights of the polymers decrease with decreasing dihedral angle. This may be due to the limited coordination options and the resulting slower growth reaction of the monomer if a constant rate of termination is assumed. In a second series of experiments (Table 3), the influence of the bridge length for *ansa*-fluorenylidene cyclopentadienylidene zirconium dichloride complexes (type B) was investigated. The bridge length was varied from one to four methylene groups. As in the case of the *ansa*-bis(fluorenylidene)zirconium dichloride complexes (type A), the bridge length of two CH_2 moieties (**11**/**12**) results in maximum catalyst activity. The reasons for the enormous catalytic potential of this complex are, as stated before, the thermal and chemical stability as well as a sufficiently large dihedral angle and an optimized electron density on the center metal atom [27]. The activities of type B metallocene complexes on silica gel/PHT are, in contrast to the type A metallocene complexes, generally, greater than the value for the analogous silica gel/MAO system. Therefore, this complex type seems to be better suited to use with the silica gel/PHT cocatalyst than the type A metallocene complexes. As before, a decrease in the molecular weight of the resulting polymers is observed as the dihedral angle is reduced.

2.4. Influence of the bridging element on the catalytic properties: copolymerization of ethylene and 1-hexene

Another focal point of this study was to elucidate the copolymerization behavior of various metallocene dichloride complexes that were each activated with both silica gel/PHT and silica gel/MAO catalyst systems. The polymerization procedure is similar to the homopolymerization of ethylene, with the exception that 1-hexene was also charged to the reactor. The reactor concentration of ethylene in the *n*-pentane phase was 0.876 mol/l, the concentration of 1-hexene was 0.133 mol/l. The polymerization results are summarized in Table 4.

The copolymerization studies with the metallocene complex type B (X = 2-hexenylidene)

Table 3
Polymerization results of different *ansa*-fluorenylidene-cyclopentadienylidene complexes activated with SiO_2/PHT and SiO_2/MAO
Polymerization conditions. SiO_2/PHT: 10.0 bar ethylene pressure, 500 ml *n*-pentane, 1.0 ml TIBA (1.6 M in *n*-hexane), 70°C, Al:Zr = 260:1, Al:O = 1.44:1, silica gel portion in the catalyst: 36%; SiO_2/MAO: 10.0 bar ethylene pressure, 500 ml *n*-pentane, 70°C, Al:Zr = 2500:1, 2.0 g SiO_2 silica gel.

Catalyst precursor/cocatalyst	Activity (kg PE/g Zr h)	PE — M_η (kg/mol)	PE — $T_{m,1}$, $T_{m,2}$ (°C)	PE — $\Delta H_{m,1}$, $\Delta H_{m,2}$ (J/g)	PE — α (%)
Type B (X = CH_2)/SiO_2/PHT (**9**)	36	460	137.1	154.2	52
Type B (X = CH_2)/SiO_2/MAO (**10**)	13	170	135.4	138.8	48
Type B (X = $(CH_2)_2$)/SiO_2/PHT (**11**)	162	350	138.6	177.2	61
Type B (X = $(CH_2)_2$)/SiO_2/MAO (**12**)	115	335	136.2	174.2	60
Type B (X = $(CH_2)_3$)/SiO_2/PHT (**13**)	32	282	138.9	166.4	57
Type B (X = $(CH_2)_3$)/SiO_2/MAO (**14**)	8.7	235	1367.7	106.1	37
Type B (X = $(CH_2)_4$)/SiO_2/PHT (**15**)	46	350	139.6	168.4	58
Type B (X = $(CH_2)_4$)/SiO_2/MAO (**16**)	95	420	139.4	181.0	62

[15] and SiO_2/PHT catalyst system show that there is a negative comonomer effect, i.e., activities decrease with 1-hexene as the comonomer. This observation is supported by the results observed for the copolymerization reactions with various metallocene dichloride complexes activated with silica gel/PHT. With the exception of **27**, all experiments with the silica gel/PHT cocatalyst systems resulted in very strong negative comonomer effects. In contrast, the silica gel/MAO catalyst system exhibits in almost all the cases a positive to a very positive comonomer effect. No correlation was found between the rate of 1-hexene insertion and the length of the bridging unit or the opening angle of the catalyst. However, *ansa*-fluorenylidene

Table 4
Copolymerization results
C5 = pentylidene.

Catalyst precursor/cocatalyst	Activity homopolymerization (kg PE/g Zr h)	T_m (°C)	ΔH_m (J/g)	Activity copolymerization (kg PE/g Zr h)	T_m (°C)	ΔH_m (J/g)	% 1-Hexene[c] in the copolymer	Comonomer effect[d]
Type B (X = CH_2)/SiO_2/PHT (**17**)[a]	36	137.1	154.2	14	119.7	81.2	15.2	− −
Type B (X = CH_2)/SiO_2/MAO (**18**)[b]	13	135.4	138.8	84	121.1	99.3	5.6	+ +
Type B (X = $(CH_2)_2$)/SiO_2/PHT (**19**)[a]	162	138.6	177.2	16	121.0	120.1	11.7	− −
Type B (X = $(CH_2)_2$)/SiO_2/MAO (**20**)[b]	115	136.2	174.2	300	123.3	109.3	6.4	+ +
Type B (X = $(CH_2)_3$)/SiO_2/PHT (**21**)[a]	32	138.9	166.4	10	126.2	120.1	7.8	− −
Type B (X = $(CH_2)_3$)/SiO_2/MAO (**22**)[b]	8.7	136.7	106.1	113	128.1	118.4	3.4	+ +
Type B (X = $(CH_2)_4$)/SiO_2/PHT (**23**)[a]	46	139.6	168.4	40	123.2	99.3	14.2	− −
Type B (X = $(CH_2)_4$)/SiO_2/MAO (**24**)[b]	95	139.4	181.0	141	128.6	126.1	6.8	+
Type A (X = 1,1-C_5)/SiO_2/PHT (**25**)[a]	34	134.3	130.8	24	127.9	89.7	5.6	−
Type A (X = 1,1-C_5)/SiO_2/MAO (**26**)[b]	114	137.1	148.0	72	124.5	87.6	12.8	−
Type A (X = $(CH_2)_2$)/SiO_2/PHT (**27**)[a]	120	139.1	165.5	160	124.1	107.2	6.3	+
Type A (X = $(CH_2)_2$)/SiO_2/MAO (**28**)[b]	275	136.4	141.5	316	123.6	105.1	3.3	+

[a] Polymerisation conditions: SiO_2–PHT: 10.0 bar ethylene pressure, 500 ml *n*-pentane, 10 ml 1-hexene, 1.0 ml TIBA (1.6 M in *n*-hexane), 70°C, Al:Zr = 260:1, Al:O = 1.44:1, SiO_2 portion in the catalyst: 36%.

[b] Polymerisation conditions: SiO_2–MAO: 10.0 bar ethylene pressure, 500 ml *n*-pentane, 10 ml 1-hexene, 70°C, Al:Zr = 2500:1, 2.0 g SiO_2.

[c] Polymerisation conditions: determined by ^{13}C and ^{1}H NMR spectroscopy.

[d] Polymerisation conditions: classification: − − very negative, − negative, + positive, + + very positive.

cyclopentadienylidene zirconium dichloride complexes (type B) exhibit in general a higher copolymerization potential than *ansa*-bis(fluorenylidene)zirconium dichloride complexes (type B). The reason for this is the better accessibility of the catalytic center in the complexes with the less bulky cyclopentadienylidene fragment compared to the fluorenylidene fragment. *Ansa*-fluorenylidene cyclopentadienylidene zirconium dichloride complexes supported on SiO_2/PHT also have higher copolymerization activities than the analogous catalyst precursors activated with SiO_2/MAO. A copolymer with short chain branches is formed due to the comonomer insertion. Therefore, the melting points of the copolymers are approximately 10%–20% below those for the homopolymers. The enthalpies of fusion decrease due to the lower crystallinity to approximately 50%. Thermal analyses of the polymers do not exhibit any trends in the thermal properties of resins made with either catalyst system.

3. Experimental section

3.1. Materials and instruments

NMR spectroscopic investigations were performed using a Bruker ARX 250 instrument. The ethylene/1-hexene copolymers were dissolved at 80°C in 1,2,4-trichlorobenzene/C_6D_6 (4:1; v/v) and measured at 80°C using ^{1}H and ^{13}C NMR spectroscopy [29–31] to determine the 1-hexene portion. The chemical shifts (δ) in ^{1}H NMR spectroscopy were referred to the residual proton signal of the solvent ($\delta = 7.15$ ppm for benzene-d_6) and in ^{13}C NMR spectroscopy to the solvent signal ($\delta = 128.0$ ppm for benzene-d_6). The thermal properties of the polymer samples were investigated for phase transitions using DSC. A NETZSCH DSC 200 instrument was available. For the measurements, 3–6 mg of the dried polymers were sealed in standard aluminum pans (Ø 5 mm) and measured under nitrogen cooling using the following temperature program: (1) Heating phase: from 60°C °C to 200°C, heating rate 20 K/min, isothermal phase (3 min), cooling phase from 200°C to 60°C, cooling rate 20 K/min. (2) Heating phase from 60°C to 200°C, heating rate 20 K/min, isothermal phase (3 min), cooling phase from 200°C to 20°C, cooling rate 20 K/min. Melting points and enthalpies of fusion were derived from heating course (2). The temperature was linearly corrected relative to indium (m.p. 156.63°C). The enthalpy of fusion of indium ($\Delta H_m = 28.45$ J/g) was used for calibration. The molecular weight determination of the polymer samples was performed using an Ubbelohde precision capillary viscometer in cis/trans decalin at 135 ± 0.1°C. The polymer samples were completely dissolved in decalin at 130°C over a period of 3–4 h. M_η was determined using calibration curves that were available for three different concentrations. All the work was routinely carried out with the help of the Schlenk technique under strict exclusion of air and moisture. Purified and dried argon was used as inert gas.

3.2. General synthesis procedure for the carrier material-PHT catalyst system

At room temperature, 30 ml of a 2.0 molar trimethylaluminum solution in toluene were added to a suspension of 2.0 g calcined silica gel (or polyethylene, $M_\eta = 310$ kg/mol) in 100 ml toluene. 0.75 ml water were transferred into another flask and a constant argon stream was passed through this flask, at last bubbling through the silica/$AlMe_3$ suspension, until all water was consumed. Thereupon, the reaction mixture heated itself to 60°C. After 10 min, the suspension became suddenly highly viscous. After cooling to room temperature, the mixture was stirred vigorously for 2 h. Finally, 0.23 mmol of the catalyst precursor was added as a solid. Depending on the solubility of the catalyst precursor, the mixture was stirred for 5–30 min, subsequently filtered and dried under high vacuum. The filtrate was colorless and con-

tained no organic or inorganic components besides the solvent. The yield of catalyst was: 5.40 g (> 95% calculated on the aluminum content) of a powder, colored according to the catalyst precursor.

3.3. Polymerization with PHT

In a 1 l round flask, 500 ml *n*-pentane with 1.0 ml trisobutylaluminum (1.6 molar solution in *n*-hexane) as the scavanger and moisture trap were mixed and stirred for 10 min. To this solution was added 0.20 g of the catalyst as a powder. The suspension was subsequently transferred into an 1 l Büchi laboratory autoclave under argon, heated to 70°C, and an ethylene pressure of 10 bar was applied (99.98% ethylene, previously dried over aluminum oxide). The amount of ethylene consumed was registered using a Büchi-Press-Flow-Control unit BPC 9901. The mixture was stirred for 1 h, and the reaction terminated by releasing the pressure from the reactor. The obtained polymer was dried under vacuum until a constant weight was achieved.

3.4. Polymerization with MAO / silica gel

About 5–10 mg of the respective catalyst precursor were weighed into a Schlenk tube and were activated with the corresponding amount of MAO (Al:Zr = 250:1). To a 1 l round bottomed flask was added 500 ml *n*-pentane, 2 g silica gel of the type ''Davison 948'' and 1.0 ml MAO-solution (30 wt.% in toluene). After 10 min, the catalyst solution prepared above was added to the mixture and stirred until the coloured metallocene complex was completely immobilized on the support. No scavanger was added, as some MAO was remaining in the pentane solution. Then, the catalyst suspension was transferred into a 1l Büchi laboratory autoclave under argon and heated to 70°C. Subsequently, an ethylene pressure of 10 bar was applied (99.98% ethylene, previously dried over aluminum oxide). After the mixture was stirred for 1 h, the reaction was terminated by releasing the pressure. The obtained polymer was dried under vacuum until a constant weight was achieved.

Acknowledgements

We thank Phillips Petroleum, Bartlesville/OK, USA, for the financial support.

References

[1] G.J. Ray, J. Spanswick, J.R. Knox, C. Serres, Macromolecules 14 (1981) 1323.
[2] E.T. Hsieh, J.C. Randall, Macromolecules 15 (1982) 353.
[3] M. Arnold, O. Henschke, J. Knorr, Macromolecules 197 (1996) 563.
[4] R. Quijada, J. Dupont, M.S.L. Miranda, R.B. Scipiori, G.B. Galland, Macromol. Chem. Phys. 196 (1995) 3991.
[5] P. Tait, I. Berry, Comprehensive Polymer Science 4 (1989) 575.
[6] F.M. Mirabella Jr., Polymer 34 (1993) 1729.
[7] H. Schwager, Kunststoffe 82 (1992) 499.
[8] L. D'Orazio, C. Mancarella, E. Martuscelli, G. Sticotti, P. Massari, Polymer 34 (1993) 3671.
[9] A. Köppl, PhD thesis, University of Bayreuth, 1998.
[10] M. Chang, Exxon Chemical, US Patent 4,912,075, 1990.
[11] G.F. Schmidt, D.A. Hucul, R.E. Campbell Jr., Dow Chemical, US Patent 5,015,749, 1991.
[12] J.A.M. Canich, G.F. Licciardi, Exxon Chemical, US Patent 5,057,475, 1991.
[13] T. Tsutsui, T. Ueda, Mitsui Petrochemical, US Patent 5,234,878, 1993.
[14] M. Chang, Exxon Chemical, US Patent 5,529,965, 1996.
[15] B. Peifer, W. Milius, H.G. Alt, J. Organomet. Chem. 553 (1998) 205.
[16] F.R. Mayo, F. Lewis, J. Am. Chem. Soc. 66 (1944) 1594.
[17] M. Fineman, S.D. Ross, J. Polym. Sci. 5 (1959) 259.
[18] H.-H. Brintzinger, D. Fischer, R. Mülhaupt, B. Rieger, R. Waymouth, Angew. Chem. 107 (1995) 1255.
[19] H.-H. Brintzinger, D. Fischer, R. Mülhaupt, B. Rieger, R. Waymouth, Angew. Chem. Int. Ed. Engl. 33 (1995) 1143.
[20] J.C.W. Chien, T. Nozaki, J. Polym. Sci. Part A: Polym. Chem. 31 (1993) 227.
[21] B. Rieger, J.C.W. Chien, Polym. Bull. 21 (1989) 159.
[22] W. Röll, H.-H. Brintzinger, B. Rieger, R. Zolk, Angew. Chem. 102 (1990) 339.
[23] W. Roll, H.-H. Brintzinger, B. Rieger, R. Zolk, Angew. Chem. Int. Ed. Engl. 29 (1990) 279.
[24] K. Soga, T. Shiono, S. Takemura, W. Kaminsky, Makromol. Chem. Rapid Commun. 8 (1987) 305.

[25] T. Tsutsui, N. Kashiwa, A. Mizuno, Makromol. Chem. Rapid Commun. 11 (1990) 565.
[26] V. Busico, R. Cipullo, P. Corradini, Makromol. Chem. Rapid Commun. 13 (1992) 15.
[27] P. Schertl, H.G. Alt, J. Organomet. Chem. 582 (1999) 328.
[28] A. Razavi, J. Atwood, Macromol. Symp. 89 (1995) 345.
[29] T. Usami, Macromolecules 17 (1984) 1756.
[30] D. Axelson, G. Levy, L. Mandelkern, Macromolecules 12 (1979) 41.
[31] J.C. Randall, Macromolecules 11 (1978) 33.